Taylor & Francis
Taylor & Francis Group

Journal of Biomolecular Structure and Dynamics

ISSN: (Print) (Online) Journal homepage: https://www.tandfonline.com/loi/tbsd20

Curcumin–silica nanocomplex preparation, hemoglobin and DNA interaction and photocytotoxicity against melanoma cancer cells

Mehrgan Ghazaeian, Khatereh Khorsandi, Reza Hosseinzadeh, Asieh Naderi & Heidi Abrahamse

To cite this article: Mehrgan Ghazaeian, Khatereh Khorsandi, Reza Hosseinzadeh, Asieh Naderi & Heidi Abrahamse (2021) Curcumin–silica nanocomplex preparation, hemoglobin and DNA interaction and photocytotoxicity against melanoma cancer cells, Journal of Biomolecular Structure and Dynamics, 39:17, 6606-6616, DOI: 10.1080/07391102.2020.1802342

To link to this article: https://doi.org/10.1080/07391102.2020.1802342

Published online: 07 Aug 2020.

JOURNAL OF BIOMOLECULAR STRUCTURE AND DYNAMICS
2021, VOL. 39, NO. 17, 6606–6616
https://doi.org/10.1080/07391102.2020.1802342

Curcumin–silica nanocomplex preparation, hemoglobin and DNA interaction and photocytotoxicity against melanoma cancer cells

Mehrgan Ghazaeian[a], Khatereh Khorsandi[b], Reza Hosseinzadeh[c], Asieh Naderi[d] and Heidi Abrahamse[e]

[a]Department of Chemistry, Faculty of Science, Islamic Azad University, North Tehran Branch, Tehran, Iran; [b]Department of Photodynamic, Medical Laser Research Center, YARA Institute, ACECR, Tehran, Iran; [c]Department of Medical Laser, Medical Laser Research Center, YARA Institute, ACECR, Tehran, Iran; [d]Department of Drug Discovery and Biomedical Sciences, College of Pharmacy, University of South Carolina, Columbia, SC, USA; [e]Laser Research Centre, NRF SARChI Chair: Laser Applications in Health, Faculty of Health Sciences, University of Johannesburg, Auckland Park, South Africa

Communicated by Ramaswamy H. Sarma

ABSTRACT

Melanoma is a malignant cancer of the skin associated with a high mortality. Early medical diagnosis and surgical intervention are essential for the treatment of melanoma. The use of plant-based compounds is an important strategy for the prevention and treatment of different types of cancers. Curcumin is a promising natural anticancer compound used towards treatment for various kinds of cancers. Studies have shown that curcumin could be applied as a photosensitizer in cancer photodynamic therapy (PDT). PDT uses light and a photosensitizing agent which produce reactive oxygen species leading to cancer cell death. The main obstacle for using curcumin as photosensitizer is its low solubilization ability in an aqueous environment. To improve its application in cancer treatment, we synthetized curcumin–silica nanoparticles as photosensitizer for photodynamic treatment of human melanoma cancer cells. Scanning electron microscopy, Transmission electron microscopy, Powder X-ray diffraction and Thermo geometric analysis indicated that curcumin was loaded on silica. The solubility of curcumin in water increased by using silica nanoparticles which wasconfirmed by spectroscopy results. The spectroscopy study confirmed the interaction of curcumin–silica nanocomplex with double strand DNA and no interaction with hemoglobin. The curcumin–silica nanocomplex and curcumin photodynamic effect was investigated on human melanoma cancer cells (A375) and also human fibroblast cells. The cell toxicity experiments showed that the curcumin–silica nanocomplex had greater photodynamic effects on cancer cell death as compared to free curcumin. The apoptotic assay by acridine orange/ethidium bromide (AO/EB) dual staining and colony forming ability confirmed the MTT results. Therefore, these results suggest that the curcumin–silica nanocomplex has great potential to be employed in photodynamic treatment of melanoma cancer.

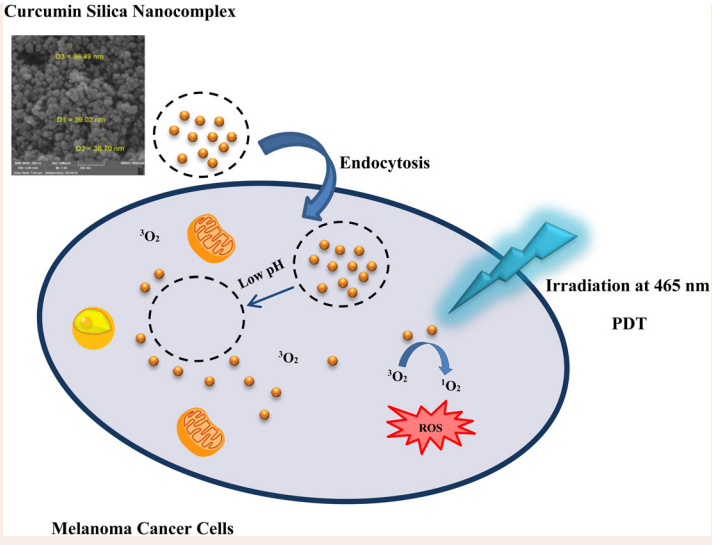

ARTICLE HISTORY
Received 13 April 2020
Accepted 23 July 2020

KEYWORDS
Curcumin–silica nanocomplex; molecular interaction; photodynamic therapy; melanoma cancer; drug delivery; apoptosis

CONTACT Khatereh Khorsandi khorsandi.kh@ut.ac.ir. Department of Photodynamic, Medical Laser Research Center, YARA Institute, ACECR, Tehran, Iran

Introduction

Skin cancer is a serious root cause of cancer deaths around the world (Siegel et al., 2019). Melanoma has the highest incidence and is the most dangerous skin cancer type, which is very common and its diagnosis is poor in advanced stages (Huang et al., 2013). Environmental factors like UV damage, as well as genetic factors, can turn the melanocytes of the skin into a cancerous melanoma (Carlson et al., 2009). Melanoma is resistant to radiation therapy and chemotherapy, hence research using alternative therapies has been well documented (Jilaveanu et al., 2009). Photodynamic therapy (PDT) is an efficient modality for different cancers that has fewer side effects than conventional treatments (Babilas et al., 2010). This method is based on a light sensitive substance that is activated at specific wavelengths of light to produce reactive oxygen species (ROS) which causes cancer cell death (Naidoo et al., 2018). Recent studies confirmed its treatment effectiveness in skin disorders such as vitiligo and psoriasis, and non-melanoma skin cancer (Babilas et al., 2010). PDT may, therefore, be a useful treatment modality for melanoma skin cancers (Ge et al., 2014; Lincoln et al., 2013; Tampa et al., 2019). This treatment has many benefits, such as low systemic aggregate toxicity, greater selectivity and noninvasive properties with the benefit of repeated treatments without serious complications. However, several causes of resistance reduce the effectiveness of PDT on melanoma cells. These mechanisms include optical interference (Hadjur et al., 1996), melanin defensive antioxidant mechanisms (Davids & Kleemann, 2010; Davids et al., 2009) and protective response through autophagy (Davids et al., 2009). Researchers are developing formulations of innovative drugs based on natural bioactive products as alternatives to chemotherapy that is typically associated with high toxicity and serious side effects (Demain & Vaishnav, 2011; Nobili et al., 2009).

Curcumin is a natural polyphenol composite from *Curcuma longa* rhizomes. Recently it was shown that curcumin has antioxidant, anti-inflammatory and anti-cancer activity (Basnet & Skalko-Basnet, 2011; Keyvani-Ghamsari et al., 2020; Xu et al., 2018). Another important property of curcumin is its activation with light which enables it to be used as a light-sensitive phototherapeutic agent in PDT (Khorsandi et al., 2015; Santezi et al., 2018). Several studies have focused on the production of curcumin nano formulations to reduce the limited use of curcumin, such as its poor solubility in water, destabilization in physiological pH and low bioavailability (Gera et al., 2017; Hosseinzadeh et al., 2018; Naksuriya et al., 2014).

The use of nanoparticles in PDT cancer treatment as a delivery system for PS drugs is progressing rapidly; these systems have many benefits, such as easy synthesis, high surface-to-volume ratio and a simple surface chemistry with high functionalization possibility (Abrahamse et al., 2017; Kruger & Abrahamse, 2018; Yi et al., 2018). Examples of PDT delivery systems involve: liposomes and micelles, ceramic, silica, polymer, metal oxide and dendrimers-based NP (Chatterjee et al., 2008; Khorsandi et al., 2019). In recent studies, silica-based nanoparticles are listed as an alternative to polymer nanoparticles (Moreno-Vega et al., 2012). Silica-based nanoparticles have special properties, such as resistance to microbes, their special shape, porosity and size which could be easily controlled during the fabrication. Silica nanoparticles can be used in PDT as they release their compounds even in unconventional pH and temperature conditions (Couleaud et al., 2010). Considering the porous membranes of silica, molecular oxygen can penetrate and reacts with the PS inside the nanoparticle. The singlet oxygen produced by light can be released from the particles and has cytotoxic effects (Xiao et al., 2011). In this study, we synthesized curcumin–silica nanocomplex (Cur–SiNPs), investigated its interaction with hemoglobin and dsDNA and evaluated its anticancer photodynamic effect against melanoma cancer (A375) and human fibroblast (HDF) as normal cell.

Materials and methods

Materials

Acridine orange (AO), ethidium bromide (EB), curcumin ($C_{21}H_{20}O_6$), 3-(4, 5-dimethylthiazol-2-yl)-2, 5-diphenyltetrazolium bromide (MTT), tryphan blue solution and dimethyl sulfoxide (DMSO) were prepared from Sigma-Aldrich (St Louis, MO, USA). Fetal bovine serum (FBS), Phosphate-buffered saline (PBS) and antibiotics were bought from Gibco (Gibco BRL). Dulbecco's Modified Eagle Medium (DMEM) was obtained from Invitrogen (Invitrogen, Carlsbad, CA, US). All the rest reagents were prepared from Merck. Calf thymus DNA (Sigma) was dissolved in deionized double distilled water then dialyzed against 10 mM Tris–HCl (pH 7.3) and stored at 4 °C. DNA concentration was determined spectrophotometrically using extinction coefficient of 20 cm^2 mg^{-1} at 260 nm.

Synthesis of curcumin–silica nanocomplex

The loading of curcumin was performed according to the batch method (El-Nahhal et al., 2018), employing an $m(SiO_2)$:m(Cur)=10:1. In brief, SiO_2 (200 mg) and curcumin (20 mg) was dissolved in PEG-400(1%) (5 mL distilled water), and then, stirred for 24 h. The solution was then centrifuged (12,000 r/min) for 10 min. In the end, the curcumin-loaded material was repeatedly washed with distilled water and dried at 50 °C overnight producing the product curcumin–silica nanocomplex. The spectrophotometric method was applied to analyse the curcumin uptake capacity on silica.

Solubility and loading efficiency of curcumin

To obtain the loading efficiency of curcumin (%) on curcumin–Si-NPs, UV/Vis spectrophotometric studies (using Cary 100 spectrophotometer) at 435 nm were done. A standard curve in the range of 0–100 μg/mL curcumin was drawn. Loading efficiency equation was used for calculating the amount of curcumin in curcumin–silica-nanoparticles (1).

$$\text{Loading efficiency}(\%) = \frac{[\text{curcumin}]_{\text{total}} - [\text{curcumin}]_{\text{free}}}{[\text{curcumin}]_{\text{total}}} \times 100 \quad (1)$$

Solubility of curcumin and curcumin–silica nanocomplex in aqueous solution was shown by dissolving them in 0.01 M of PBS in pH 7.4, separately. For this purpose, the specific amount of both curcumin and curcumin–silica nanocomplex (100 μg/mL) were stirred for 5 min. The A_{max} of each sample were obtained measuring maximum absorbance. The enlargement of curcumin solubility in nanoparticles can be obtained as A_{max}-Curcumin–silica nanocomplex/A_{max} curcumin.

Characterization of curcumin–silica nanocomplex

The absorption spectrum of curcumin–silica nanocomplex was assessed using UV/Vis spectrophotometer Cary 100, equipped with quartz cuvettes. Powder X-ray diffraction (XRD) patterns were obtained by Rigaku Miniflex X-ray diffractometer using CuKα radiation ($\lambda = 0.154$ nm). The morphology of nanoparticles was determined by transmission electron microscope (TEM) and scanning electron microscope (SEM).

Thermal gravimetric analysis

Thermal gravity analysis (SDT Q600, from TA Instruments Co) was used. The percentage of curcumin loading on silica nanoparticles was determined by thermal gravimetric analysis (TGA). The thermal weight losses were recorded by increasing of temperature up to 800 °C by the ramp of 5 °C/min.

Human adult hemoglobin extraction

Purified human hemoglobin (Hb) was extracted from healthy, nonsmokers according to the A. Riggs method (Hosseinzadeh & Moosavi-Movahedi, 2016; Riggs, 1981). Briefly, fresh and heparinized blood was centrifuged at 3000 rpm. The packed red blood cells were washed three times with isotonic saline solution (0.9% NaCl) and centrifuged at 10,000 rpm for 5 min at a ratio of 1:10 to remove the yellowish solution. Cold double distilled water was used for lysing red blood cells to prevent slow oxidation. The membrane components were removed by centrifugation at 10,000 rpm. To remove any insoluble materials, the soluble Hb was centrifuged two additional times at 18,000 rpm. The $(NH_4)_2SO_4$ was added to Hb solution to obtain the 20% saturation then was centrifuged for 20 min at 20,000 rpm. Hb solution was dialyzed 3 times with 0.2 M phosphate buffer (pH = 7.4) for 24 h (Riggs, 1981).

UV/Vis spectroscopy

The UV/Vis spectrum of DNA and hemoglobin was obtained using a UV–Visible spectrophotometer (Cary 100 UV/Vis) equipped with 1.0 cm quartz cells. The UV absorption spectra of 4 μg/mL of hemoglobin protein and 100 μg/mL and DNA was incubated individually at different concentrations of curcumin–silica-NPs at room temperature for 45 min and then scanned at a range of 200–800 nm.

Cell line and culture

Human melanoma cancer (A375) and human dermal fibroblast (HDF) cell lines were purchased from the Institute of Pasture, Tehran, Iran. The cells were grown in DMEM medium supplemented with 10% FBS, 100 IU mL^{-1} penicillin and 100 μg mL^{-1} of streptomycin and then kept in a humidified incubator containing 5% CO_2 at 37 °C. The cells were removed by trypsinizing (trypsin 0.025%, EDTA 0.02%) and washed with PBS for all cellular experiments.

Photodynamic treatment: in vitro study

At 80–90% confluence of A375 and HDF cells, the cells were washed with PBS, and then, detached from the flask by adding 1.0 mL of 0.25% trypsin for 1 – 3 min at 37 °C. The 10^4 cells/well were seeded into two 96-well plates. The cancer and normal cells were treated with curcumin–silica-NPs and free curcumin at different concentrations (0, 10, 25, 50 and 100 μg/mL) for 4 and 24 h. In another experiment for finding the effect of antioxidant on PDT, the A375 cells were incubated with curcumin–silica-NPs as PS and after the incubation time (24 h), rinsed with PBS, then, incubated for 30 min with ascorbate. Before exposure to light, the cells were rinsed again with PBS. In these experiment, one plate was incubated in the dark for 15 min and another was irradiated for 15 min with a blue LED (465 nm; power density: 34 mW/cm^2) at room temperature (25 °C). The cell viability analyzed by MTT method. All experiments were done at least 3 times.

Photocytotoxicity

The MTT assay was used for determining cell viability as ability of cells redox capacity. Living cells could turn the MTT compound to an insoluble formazan which can be solubilized using dimethyl sulfoxide (DMSO) and its concentration was determined by spectrophotometric assay. In brief, culture medium was removed and the cells were incubated in medium containing 0.5 mg/mL of MTT solution for 3–4 h at 37 °C. Then, the resulting purple formazan crystals dissolved in 100 μL DMSO and shacked for 15 min. The solutions absorbance was determined at 570 nm by an ELISA reader (Hyperion, Inc., FL, USA). Each experiment was done at least three times. The data are shown as the mean ± *SD*.

Clonogenic assay

The ability of A375 cells colony forming was evaluated after treatment with curcumin–silica NPs-PDT. For this purpose after treating s, the cancer cells were gathered by trypsinization and total numbers of cells were counted and 200 cells/plate were seeded. After one week of incubation at 37 °C, colonies were stained with 0.5% crystal violet in methanol and the number of colonies was counted. The control was considered as untreated cells kept for 24 h.

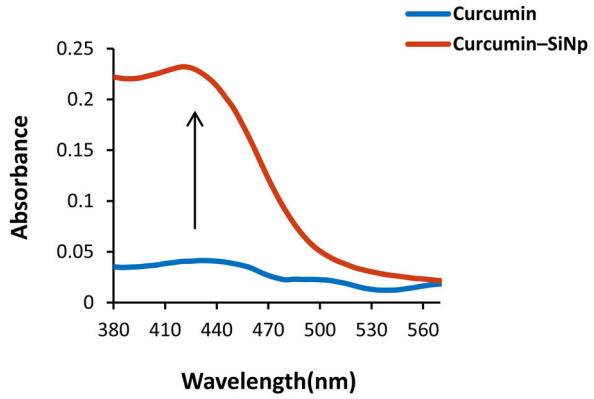

Figure 1. The UV–Vis spectra of free curcumin (blue line), and curcumin–Si nanocomplex (orange line) in aqueous solution.

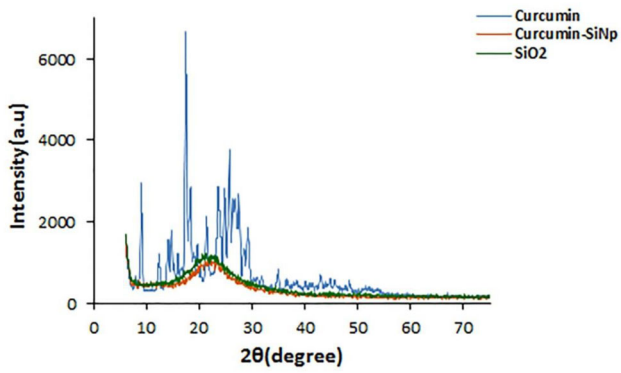

Figure 2. X-ray diffraction patterns of curcumin–Si nanocomplex (orange), pristine curcumin (blue) and silica particles (green).

Determination of apoptotic/necrotic cells: dual AO/EB fluorescent staining

Photodynamic treatment mediated curcumin–silica NPs could induced morphological changes which were discovered by fluorescence microscopy using AO/EB staining. The treated A375 cells were pelleted and resuspended in 100 μL of PBS then stained with AO/EB. The concentrations of EB (E7637; Sigma) and AO (A6014) were 0.25 and 0.1 mM, respectively. All samples were examined at room temperature immediately.

Evaluation of ROS generation in the cells

The intracellular accumulation of reactive oxygen molecules (ROS) was determined by the 7.2-dichlorofluorosine diacetate (DCFH2-DA) assay. For this purpose, The A375 cells were cultured at approximately 10^6 cells per petri dish. Cells were treated with 0 and 50 μg/mL of curcumin–Si NP then irradiated at 660 nm for 15 min (PDT). After that cell culture medium was removed and the cells were incubated with 2 mM DCFH2-DA for 45 min in the dark. The cells were then washed with PBS and transferred to a flow cytometer for ROS measurment. The data from flow cytometry were analyzed with FlowJo 7.6.1 software and related charts are presented in the results section.

Statistical analysis

Statistical analysis was executed with Student's *t*-test (two tailed). All data are shown as means ± *SD*. Results are defined as *n* denoting the number of experiments. $p < .05$ was referred to statistically significant.

Results

Curcumin–Si nanocomplex physicochemical analysis

The solubility of curcumin in aqueous solution was increased up to 5 in nanoparticle. The efficiency of curcumin loaded on silica was found about 5%. Figure 1, shows the absorption spectrum of curcumin–Si nanocomplex and bare curcumin in aqueous solution. The absorption spectrum of curcumin–Si nano indicated an absorbance peak at 425 nm, an increase of 0.18 units compared to the bare curcumin

Structural and morphological characterization

Figure 2 demonstrates the XRD patterns of synthesized nanocomplexes. The diffraction pattern displayed curcumin had two sharp peaks at $2\theta = 8.78^\circ$ and 17.16°, and additional peaks of lower intensity. The absence of these characteristics reflections in curcumin–Si nanocomplex demonstrated the loading of curcumin on the silica structure.

TEM (Figure 3(A)) and SEM (Figure 3(B)) images indicates that the curcumin–Si nanocomplexes have uniform shape with particle sizes varying from 36 to 40 nm. The SEM, TEM and XRD results confirmed the UV/Vis spectrophotometry results about curcumin–Si nanocomplex synthesis.

TGA charts related to bare curcumin, SiO_2 and curcumin–Si nano complex (Figure 4). The TGA exhibited that curcumin loaded on silica about 5% loading was achieved. The results are in accordance with spectrophotometric measurement results. It means that the final concentration of curcumin in nanoparticles is approximately 2.5 μg/mL. For example at 50 μg/mL of curcumin–Si nanoparticle the concentration of curcumin in the nanocomplex in comparison to free curcumin is 1:20.

UV/Vis spectroscopy of curcumin–Si nanocomplex interaction with hemoglobin and DNA

UV/Vis spectrum of free Hb shows three main peaks in the range of 200–700 nm. The first peak at 220–280 nm related globin, the second peak due to the Heme (prosthetic group) as a Soret or S band at 360–450 nm and third one at 500–580 nm as a oxy- and deoxy-form of Heme (Q band) (Chatterjee & Kumar, 2016; Messori et al., 2006). The Heme group is a Fe-porphyrin complex that bur in the hydrophobic pocket of globin which leads to strong Soret peak at 406 nm. Changes in the absorbance at absorbance peak are due to structural alternations in the native Hb form. As shown in Figure 5, addition of nanocomplex caused hypochromism in thr Soret band without red or blue shifts, mainly due to the non-exposure of Heme system from the crevices to the exterior part of the subunit.

UV/Vis spectroscopy is a reliable method to examine the binding mode of DNA with various molecules. The absorbance spectrum of DNA shows hypochromism and hyperchromism due to compounds binding to DNA and

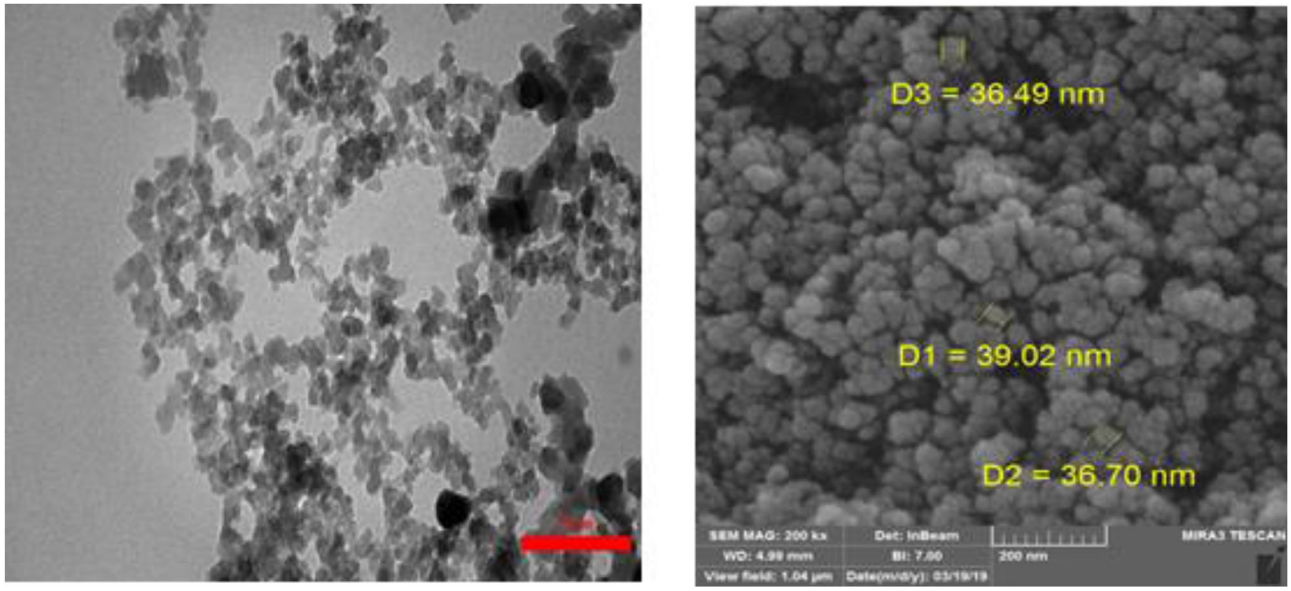

Figure 3. The SEM (A) and TEM (B) images of the curcumin–Si nano complex.

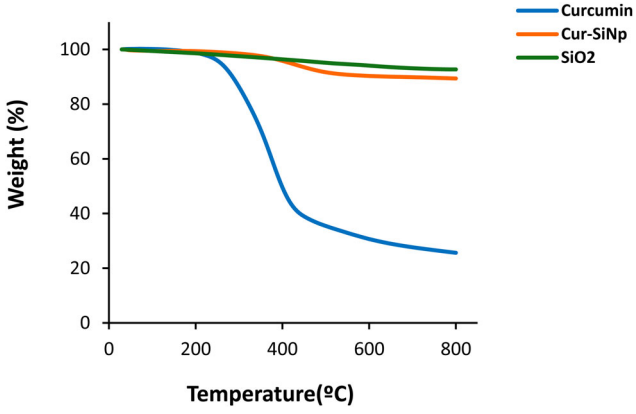

Figure 4. TGA curves for curcumin–Si nanocomplex (orange), pristine curcumin (blue) and silica particles (green).

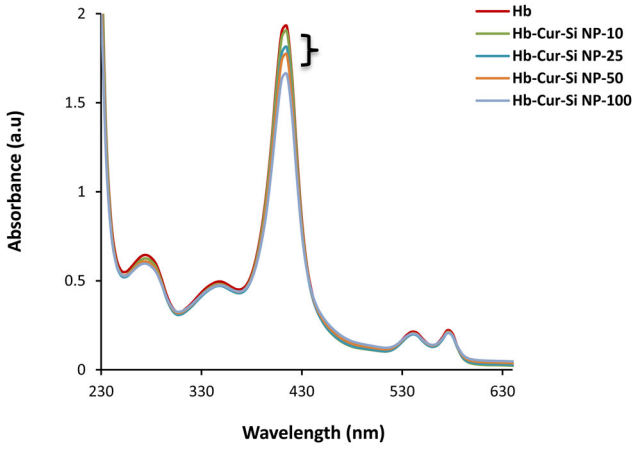

Figure 5. UV–Visible spectra of hemoglobin in the presence of different concentrations of curcumin–Si nanocomplex (0, 10, 25, 50 and 100 µg/mL). The results are expressed as the mean ± *SD* ($n = 3$, $p < .005$).

consequently double-helix structural changes. Therefore, in order to investigate the possibility of binding of curcumin–-silica nanocomplex to double strand DNA, spectroscopic of the DNA in presence of different concentration of

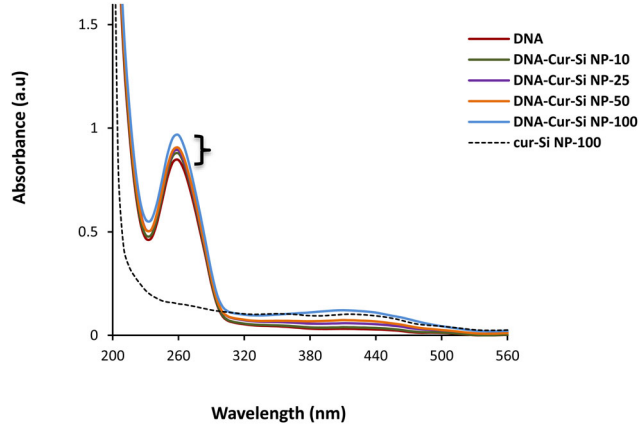

Figure 6. UV–Visible absorption spectra of DNA (50 µg/mL) in the presence of increasing concentrations of curcumin–Si nanocomplex (0, 10, 25, 50 and 100 µg/mL) in Tris-HCl buffer (pH 7.4). Hyperchromism confirmed the interaction of curcumin–Si nanocomplex and DNA. The results are expressed as the mean ± *SD* ($n = 3$, $p < .005$).

curcumin–Si nanocomplex was performed. The hyperchromism means the breakage of the secondary structure of DNA; the hypochromism is due to the stabilization of the DNA double helix by either the intercalation binding mode or the electrostatic effect of small molecules (Tu et al. 2015). The effect of curcumin–Si nanocomplex on DNA UV–Vis absorption spectrum is shown in Figure 6, as it can be seen upon increasing the curcumin–Si nanocomplex concentration, the absorption spectra of DNA at 260 nm (which is related to base pairs of DNA) increases (hyperchromism) with no apparent shift in maximum absorption peak.

Curcumin–Si nanocomplex photo cytotoxicity on A375 melanoma cancer and human normal fibroblast cells

To explore the cytotoxicity of curcumin–Si nanocomplex after PDT with blue light irradiation, the A375 human melanoma cancer cells was treated with different concentrations of curcumin and curcumin–Si nanocomplex (0,10, 25, 50 and

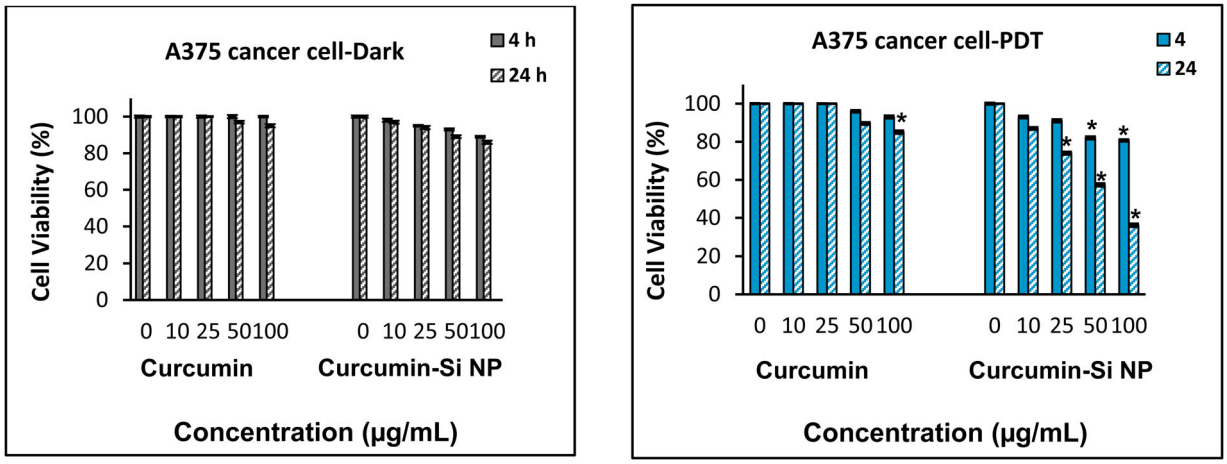

Figure 7. The dark and PDT toxicity of curcumin and curcumin–Si nanocomplex at different concentrations at 4 h and 24 h incubation on A375 melanoma cancer cells. The results are expressed as the mean ± *SD* ($n = 3$, $^*p < .05$ compared with the control (untreated) group).

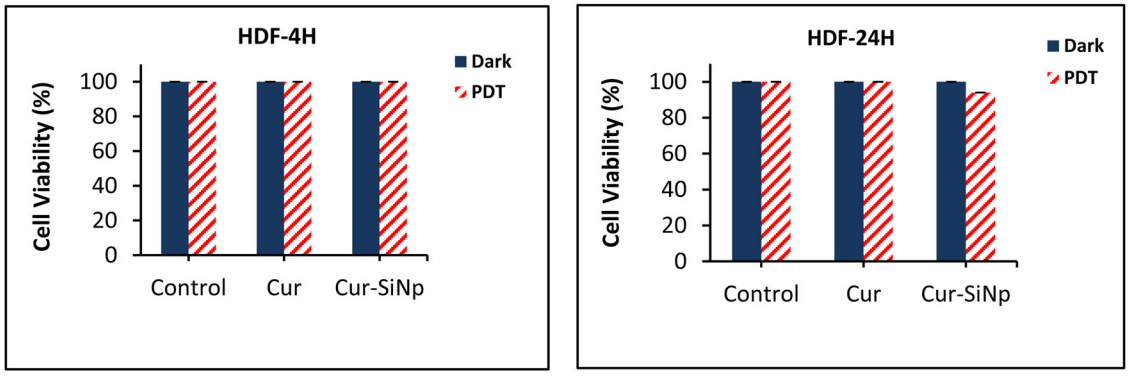

Figure 8. The PDT effect of curcumin (Cur) and curcumin–Si nanocomplex (Cur–SiNP) at 50 µg/mL (IC_{50}) on human dermal fibroblast (HDF) after 4 h and 24 h incubation. The results are expressed as the mean ± *SD* ($n = 3$, $^*p < .05$ compared with the control (untreated) group).

100 µg/mL) for 4 and 24 h. For human dermal fibroblast cells the same experiment was done but at IC_{50} of curcumin–Si nanocomplex. Then one plate of treated cells was illuminated with a blue LED (465 nm; power density: 34 mW/cm^2) and another was kept in the dark for 15 min. After 24 h, the cells were studied for cell toxicity by MTT solution. As shown in Figure 7, curcumin–Si nano -PDT induced cytotoxicity in A375 cells but not in human normal fibroblast (Figure 8). As it seen in Figure 7, the viability of curcumin–Si nanocomplex treated cells with 50 µg/mL of curcumin–Si nanocomplex after 24 h at dark condition was more than 90% ($p > .05$). After PDT the cell viability reached to 57% ($p < .05$) which is more than the photocytotoxicity of alone curcumin (89%; $p < .05$). It's interesting that low amount of curcumin in nanocomplex (about 2.5 µg/mL) than free curcumin (50 µg/mL) showed better PDT efficacy and its phototoxicty effect was increased by using silica as nano vehicle for delivery of curcumin to melanoma cancer cells.

The results show that with irradiation the cell viability of control sample (only PBS) has not significant changes confirm that the used dosage of light does not show phototoxicity on normal and cancer cells in the absence of photosensitizers (Figures 7 and 8). These results suggest that curcumin–Si nanocomplex after PDT with blue light could show cytotoxic effect against A375 melanoma cell. The data demonstrate as the mean ± *SD* of the three equal experiments each done in triplicate.

Curcumin–Si nanocomplex-PDT effect on cell proliferation of A375 melanoma cells

The colony forming ability of A375 melanoma cells treated with curcumin–Si nanocomplex then PDT (Figure 9(D)) decreased compared to other groups including 0 µg/mL at dark (Figure 9(A)), 50 µg/mL of curcumin–Si nanocomplex at dark (Figure 9(B)) and 0 µg/mL with irradiation (Figure 9(C)). The ability of melanoma cancer cells in colony forming at 0 µM of sample (dark (Figure 9(A)) and irradiation (Figure 9(C)) groups did not changes; this implies that blue light irradiation could not impact the ability of the cells in colony formation but along with curcumin–Si nanocomplex (50 µg/mL) could reduce it.

Apoptosis detection

The cells in the untreated group (control-dark) (Figure 10(A)) and the cells treated with 0 µg/mL of curcumin–Si nanocomplex and irradiated with blue LED (control-irradiation) (Figure 10(C)), are green and have round-shapes with intact nuclei. Following treatment with curcumin–Si nanocomplex the cells turn to red (early or late apoptotic cells) with fragmental or condensed

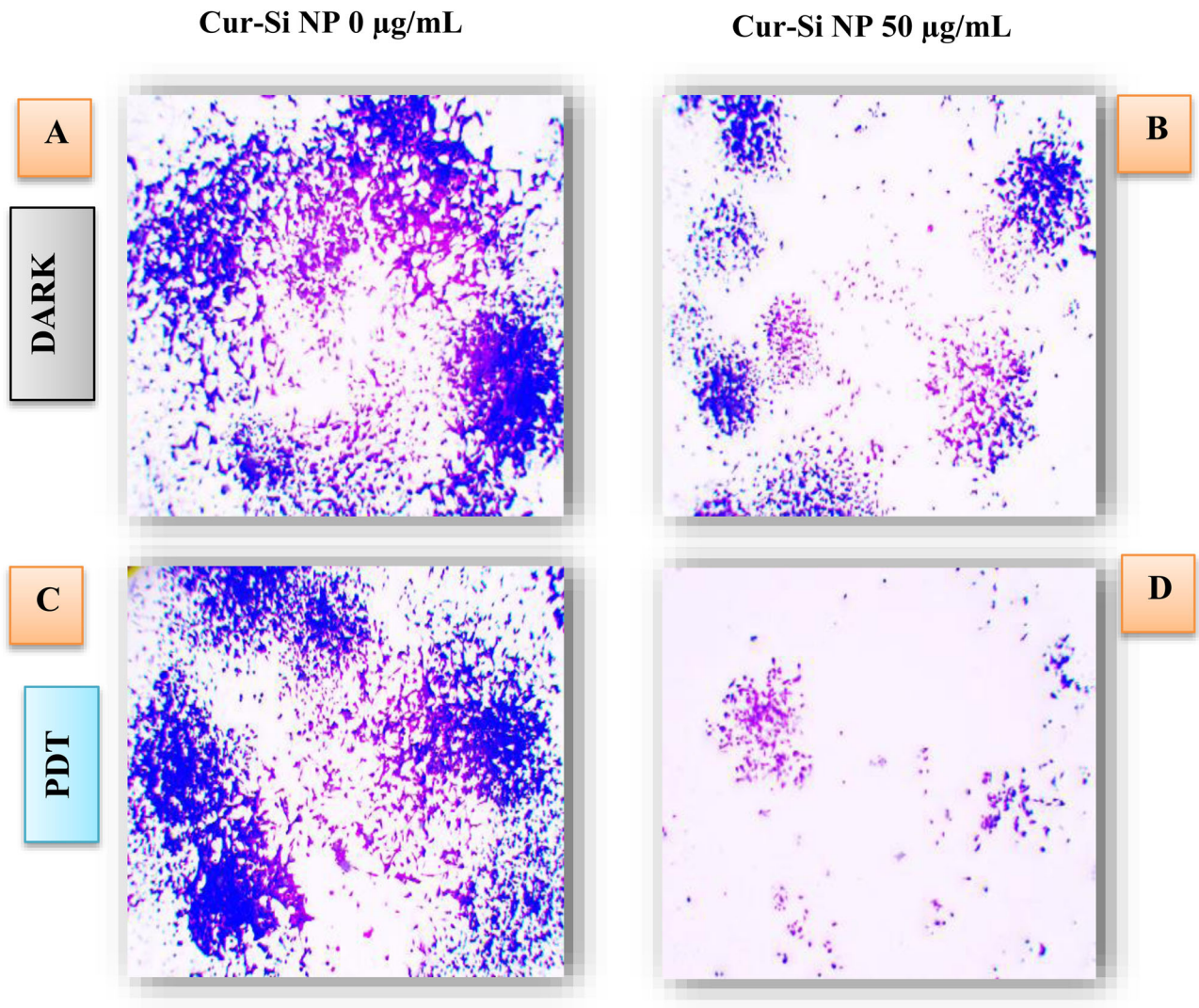

Figure 9. Clonogenic assay images (10×) of A375 melanoma cancer cells after treatment with (0 µg/mL (A) and 50 µg/mL (B) of curcumin–Si nanocomplex at dark condition and at (0 µg/mL (C) and 50 µg/mL (D) of curcumin–Si nanocomplex under irradiation with blue light (PDT).

nuclei (Figure 10(B)). As it can be seen, upon incubation with curcumin–Si nanocomplex then irradiated (PDT; Figure 10(D)) the late apoptotic and necrotic cells were increased.

ROS generation after photodynamic treatment with curcumin–Si nanocomplex

As illustrated in Figure 11, the A375 melanoma cancer cells indicated enhanced ROS generation after treatment with 50 µg/mL of curcumin–Si nanocomplex then PDT (D) in comparison to the dark control group (A), 50 µg/mL of curcumin–Si NP at dark (B) and control irradiation (0 µg/mL of curcumin–Si NP) (C) groups. It indicates that ROS production could be one of the possible mechanisms of cell death induction in the A375 melanoma cancer cells after curcumin–Si NP treatment followed by PDT.

Photodynamic effect of curcumin–Si nanocomplex in presences of ascorbate

In this experiment, ascorbate was incubated for 30 min before PDT; as it noted, this is enough time for cell uptake, but not much for ascorbate to be degraded or reduced by metal ions in the environment(Grimm et al., 2011). In order to investigate the combination of PDT with ascorbate, we selected IC_{50} dose of curcumin–Si nanocomplex. As it can be seen in Figure 12, ascorbate as an antioxidant protects A375 form ROS generation during PDT with curcumin–Si nanocomple. It means that the cell viability of A375 cells recovered in the presence of antioxidant.

Discussion

There are several common cancer therapies such as chemotherapy, surgery and radiation or combination for melanoma cancer. Various studies have been performed to improve the efficiency of PDT against melanoma. The PS excitation produces cytotoxic ROS such as singlet molecular oxygen, superoxide anions and/or hydroxyl radicals that lead to phototoxic effect on cancer cells through oxidative stress (Castano et al., 2005; Palumbo, 2007). PDT is a potential modality for melanoma treatment, and much knowledge has been gained from extensive research over the past years, but further research is

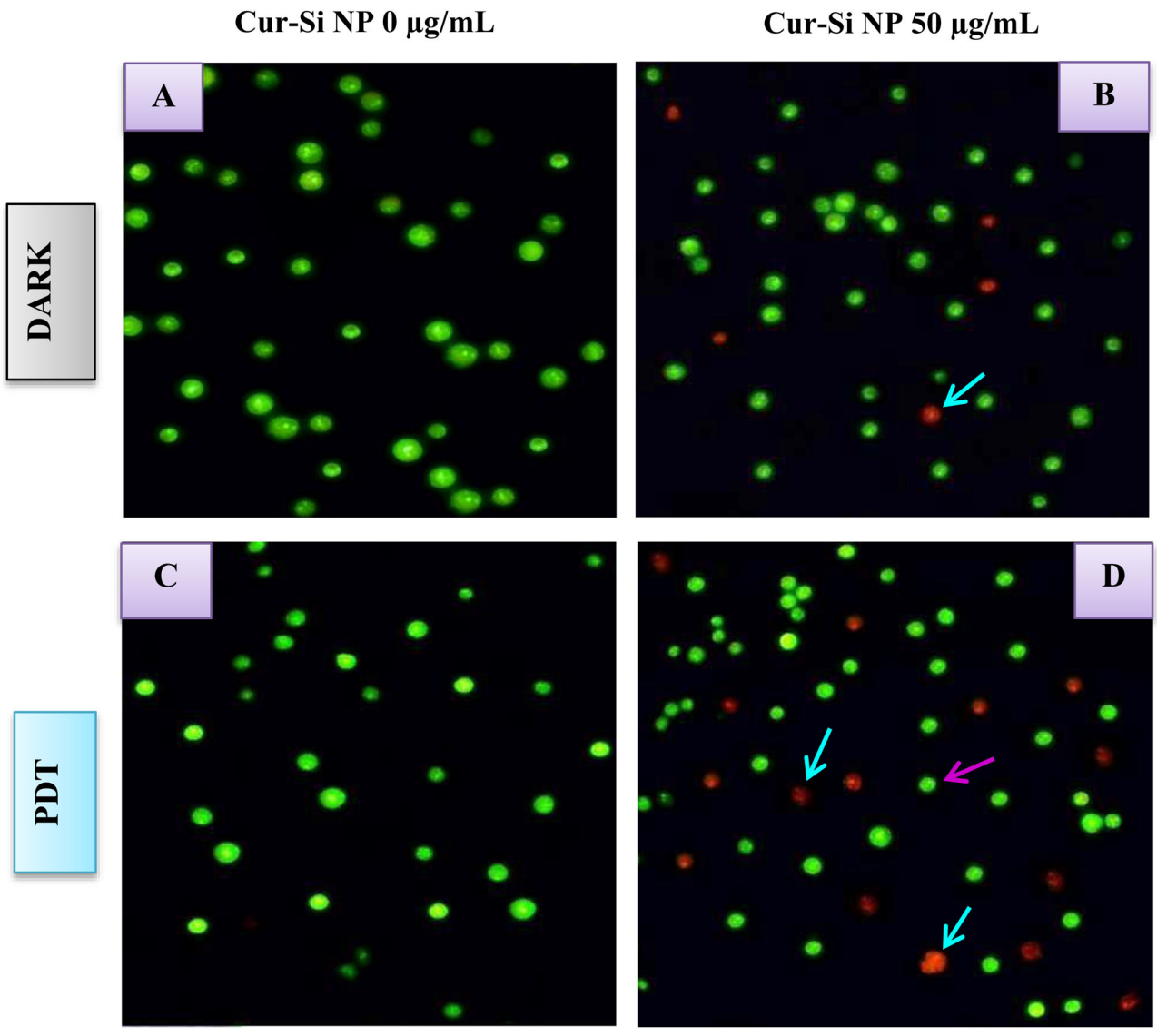

Figure 10. Fluorescence microscopic images (10×) of apoptosis induction by curcumin–Si nanocomplex-PDT using AO/ED dual staining of A375 cells after treatment with (0 µg/mL of curcumin–Si nanocomplex (A) and 50 µg/mL (B) of curcumin–Si nanocomplex at dark condition and 0 µg/mL (C) and 50 µg/mL (D) of curcumin–Si nanocomplex under irradiation with blue light (PDT). Normal cells are uniformly green, early apoptotic cells are green with bright green dots in their nuclei as a result of chromatin condensation and nuclear fragmentation. Late apoptotic/necrosis cells are orange to red.

needed to overcome melanoma resistance. The effectiveness of curcumin is relatively low mainly due to its poor solubility in water. To resolve these limitations, various studies have focused on the preparation of curcumin as nanoformulations (Khorsandi et al., 2019; Verwanger et al., 2011). Here, we designed the experiment towards synthesis and application of curcumin–silica nanocomplex for use in photodynamic treatment of A375 melanoma cancer cells.

As mentioned the absorbance of free curcumin is low due to its poor solubility in water and hydrophobic structure. However, when curcumin is loaded on silica structures, its absorbance peak increased. The increase of the curcumin–silica absorbance peak indicated that the curcumin on silica structures was well distributed in solution. In addition, experiments have been done to demonstrate the successful synthesis of curcumin–silica nanocomplexs including SEM, TEM and XRD techniques. It can be seen from the XRD result that bare curcumin hides its crystallinity after loading and also the intensity of corresponding peaks decreased. Hence, we propose that the curcumin loaded on silica nanoparticles as indicated in results obtained from the TEM and SEM data confirmed the XRD results. TGA analysis showed that silica nanoparticles (blue curve) do not exhibit significant weight loss up to 800 °C. The TGA graph for bare curcumin (orange curve) exhibits rapid weight loss in the range of 270–445 °C which may be based on the degradation of curcumin. The curcumin–silica nanocomplex also starts to lose weight at 350 °C to 500 °C with slow rate and subsequently it becomes slower. The results of TGA display that approximately 5% of curcumin was loaded in silica nanoparticles. It can, thus, be concluded that about 2.5 µg/mL of curcumin is in curcumin–Si nanocomplexes. It means that the ratio of curucmin in nanocomplex to free curcumin is 1:20.

The spectroscopic study on the interaction of curcumin–Si nanocomplex with Hb revealed no shift in the Soret band and no significant changes in the globin and Q bands of Hb

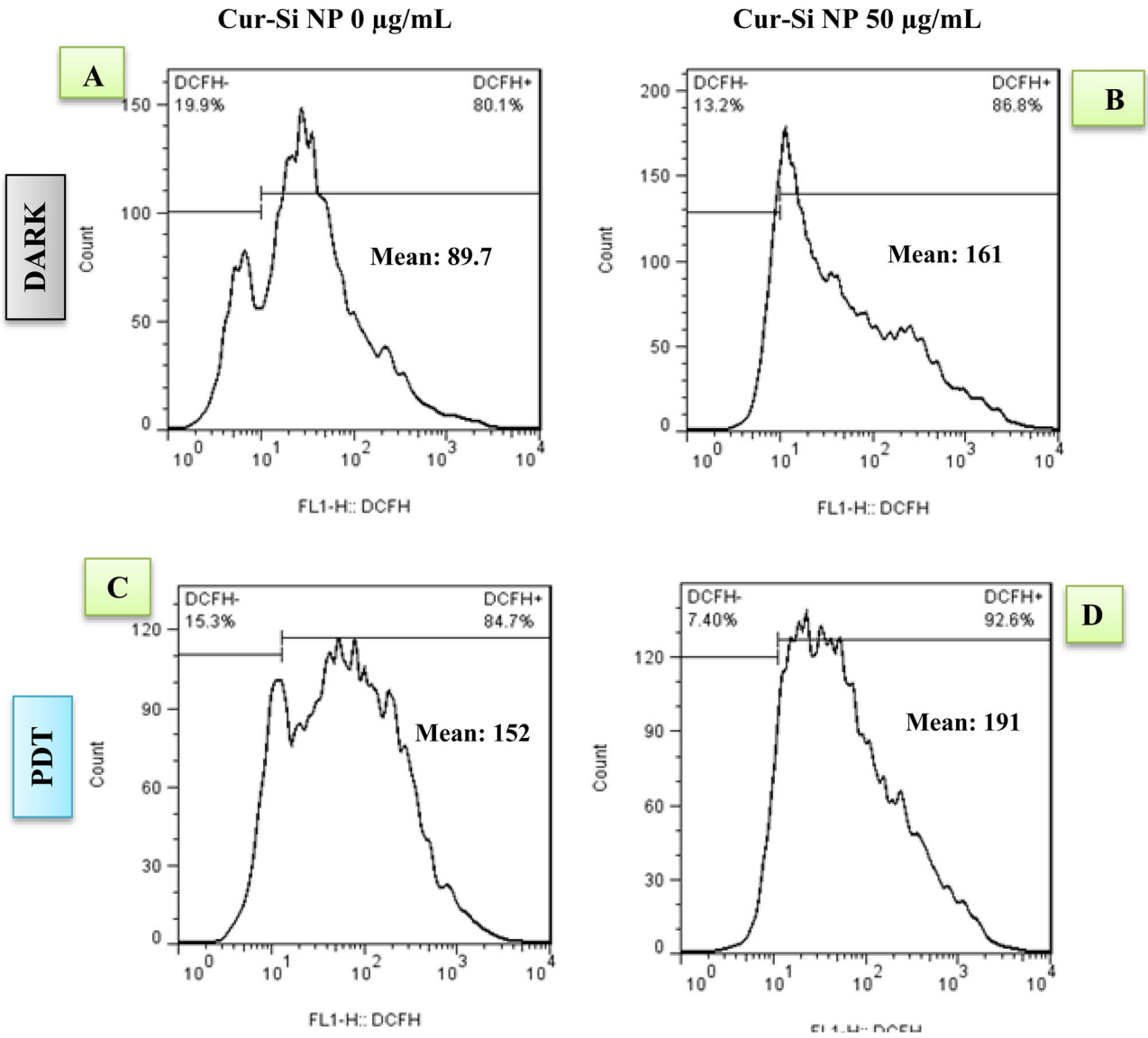

Figure 11. Effects of I curcumin–Si NP then irradiation with blue light (PDT) on intracellular ROS generation in A375 melanoma cancer cells. Dark control group (A), 50 µg/mL of curcumin–Si NP at dark (B) control irradiation (0 µg/mL of curcumin–Si NP) (C) and 50 µg/mL of curcumin–Si NP and PDT. The cells were stained with DCFH-DA (2 mM), followed by flow cytometry.

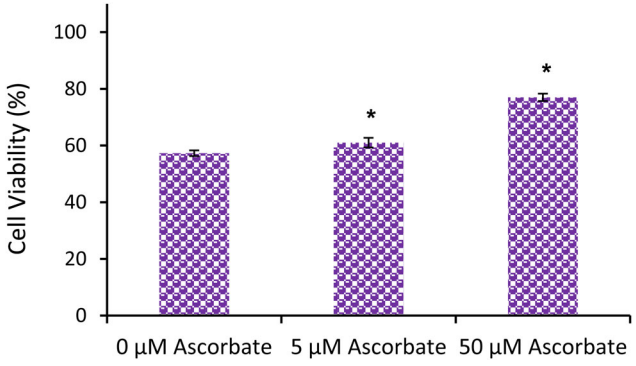

Figure 12. phototoxicity of curcumin–Si nanocomplex (50 µg/mL) for 24 h alone or in combination with ascorbate (5 µ M and 50 µM). Ascorbate acts as an antioxidant with A375 melanoma cancer cell. The results are expressed as the mean ±*SD* ($n = 3$, $^{*}p < .05$ compared with the control (without ascorbat group).

indicating that curcumin–Si nanocomplex retain the biological function of hemoglobin. In other words, hypochromic changes of the Soret band without any shift are due to weak molecular interactions between nanocomplexes and hemoglobin hydrophobic pockets because of the hydrophobic nature of curcumin on the surface of silica particles. These interactions are weak and do not have any significant structural changes in hemoglobin. This experiment revealed that the nanocomplexes have not toxic effect on Hb structure and function (Figure 5).

The increase in absorbance (hyperchromism) in DNA spectrum at 260 nm suggest curcumin–Si nanocomplexes bind to DNA resulting in reduction in the base stacking interaction and consequently an increase in their absorption (Nafisi et al., 2009; Sweeting, 1998).

The results of photocytotoxicity of curcumin–Si nanocomplex against melanoma and normal cells represents low cytotoxicity of the nanocomplex on the HDF cells while potential toxic effect against melanoma cancer cells. The apoptotic cell's features by fluorescent staining are nuclear fragmentation and chromatin condensation that can be observed after photodynamic treatment with curcumin–SiNp at 50 µg/mL.

The prominent feature of cancer cells is unmanageable cell proliferation. Thus, inhibition of cancer cell proliferation is an essential tool for regulating cancer cells. Our results demonstrated that the A375 cells proliferation ability under curcumin–silica-PDT was reduced and a few colonies can be considered at IC_{50} of curcumin–silica (50 μg/mL) after PDT. The results showed that when curcumin was used in nanoformulations with low concentrations of free curcumin (1:20) it showed better photodynamic effects than free curcumin. In the PDT process, the excited PS transfers energy to molecular oxygen and generates ROS which is cytotoxic and could lead to oxidative damage or cell death in cancer cells. Our results suggest that curcumin–Si nanocomplex in conjunction with PDT could induce growth inhibition and also apoptosis through enhancing intracellular ROS (as it confirmed in presence of antioxidant also flowcytometry assay). The results are consistent with other research showing that curcumin exhibits phototoxic effects on cancer cells (Bernd, 2014; Duse et al., 2019; Gangwar et al., 2013; Khorsandi et al., 2019; Paunovic et al., 2016; Singh et al., 2015).

Conclusion

This study reports that the solubility of curcumin is increased in curcumin–silica noncomplexes and PDT with blue LED irradiation could enhance the cell toxicity effect of curcumin even at low concentrations in nanocomplex form. This result offers a new viewpoint on human melanoma cancer PDT. However, a lot of questions regarding signaling pathways remain unknown and more work is required to elucidate exact mechanisms.

Acknowledgement

The authors thank people who helped them to perform this research.

Disclosure statement

No potential conflict of interest was reported by the authors.

ORCID

Khatereh Khorsandi http://orcid.org/0000-0001-6882-5031

References

Abrahamse, H., Kruger, C. A., Kadanyo, S., & Mishra, A. (2017). Nanoparticles for advanced photodynamic therapy of cancer. *Photomedicine and Laser Surgery*, *35*(11), 581–588. https://doi.org/10.1089/pho.2017.4308

Babilas, P., Schreml, S., Landthaler, M., & Szeimies, R.-M. (2010). Photodynamic therapy in dermatology: State-of-the-art. *Photodermatology, Photoimmunology & Photomedicine*, *26*(3), 118–132. https://doi.org/10.1111/j.1600-0781.2010.00507.x

Basnet, P., & Skalko-Basnet, N. (2011). Curcumin: An anti-inflammatory molecule from a curry spice on the path to cancer treatment. *Molecules*, *16*(6), 4567–4598. https://doi.org/10.3390/molecules16064567

Bernd, A. (2014). Visible light and/or UVA offer a strong amplification of the anti-tumor effect of curcumin. *Phytochemistry Reviews*, *13*(1), 183–189. https://doi.org/10.1007/s11101-013-9296-2

Carlson, J. A., Ross, J. S., & Slominski, A. J. (2009). New techniques in dermatopathology that help to diagnose and prognosticate melanoma. *Clinics in Dermatology*, *27*(1), 75–102. https://doi.org/10.1016/j.clindermatol.2008.09.007

Castano, A. P., Demidova, T. N., & Hamblin, M. R. (2005). Mechanisms in photodynamic therapy: Part two – Cellular signaling, cell metabolism and modes of cell death. *Photodiagnosis and Photodynamic Therapy*, *2*(1), 1–23. https://doi.org/10.1016/S1572-1000(05)00030-X

Chatterjee, D. K., Fong, L. S., & Zhang, Y. (2008). Nanoparticles in photodynamic therapy: An emerging paradigm. *Advanced Drug Delivery Reviews*, *60*(15), 1627–1637. https://doi.org/10.1016/j.addr.2008.08.003

Chatterjee, S., & Kumar, G. S. (2016). Binding of fluorescent acridine dyes acridine orange and 9-aminoacridine to hemoglobin: Elucidation of their molecular recognition by spectroscopy, calorimetry and molecular modeling techniques. *Journal of Photochemistry and Photobiology. B, Biology*, *159*, 169–178. https://doi.org/10.1016/j.jphotobiol.2016.03.045

Couleaud, P., Morosini, V., Frochot, C., Richeter, S., Raehm, L., & Durand, J.-O. (2010). Silica-based nanoparticles for photodynamic therapy applications. *Nanoscale*, *2*(7), 1083–1095. https://doi.org/10.1039/c0nr00096e

Davids, L. M., & Kleemann, B. (2010). Combating melanoma: The use of photodynamic therapy as a novel, adjuvant therapeutic tool. *Cancer Treatment Reviews*. Retrieved from https://doi.org/10.1016/j.ctrv.2010.11.007

Davids, L. M., Kleemann, B., Cooper, S., & Kidson, S. H. (2009). Melanomas display increased cytoprotection to hypericin-mediated cytotoxicity through the induction of autophagy. *Cell Biology International*, *33*(10), 1065–1072. https://doi.org/10.1016/j.cellbi.2009.06.026

Demain, A. L., & Vaishnav, P. (2011). Natural products for cancer chemotherapy. *Microbial Biotechnology*, *4*(6), 687–699. https://doi.org/10.1111/j.1751-7915.2010.00221.x

Duse, L., Agel, M. R., Pinnapireddy, S. R., Schäfer, J., Selo, M. A., Ehrhardt, C., & Bakowsky, U. (2019). Photodynamic therapy of ovarian carcinoma cells with curcumin-loaded biodegradable polymeric nanoparticles. *Pharmaceutics*, *11*(6), 282. https://doi.org/10.3390/pharmaceutics11060282

El-Nahhal, I. M., Salem, J. K., & Tabasi, N. S. (2018). Uptake of curcumin by supported metal oxides (CaO and MgO) mesoporous silica materials. *Journal of Sol-Gel Science and Technology*, *87*(3), 647–656. https://doi.org/10.1007/s10971-018-4763-2

Gangwar, R. K., Tomar, G. B., Dhumale, V. A., Zinjarde, S., Sharma, R. B., & Datar, S. (2013). Curcumin conjugated silica nanoparticles for improving bioavailability and its anticancer applications. *Journal of Agricultural and Food Chemistry*, 61(40):9632-9637. Retrieved from https://doi.org/10.1021/jf402894x

Ge, J., Lan, M., Zhou, B., Liu, W., Guo, L., Wang, H., Jia, Q., Niu, G., Huang, X., Zhou, H., Meng, X., Wang, P., Lee, C.-S., Zhang, W., & Han, X. (2014). A graphene quantum dot photodynamic therapy agent with high singlet oxygen generation. *Nature Communications*, *5*(1), 4596. https://doi.org/10.1038/ncomms5596

Gera, M., Sharma, N., Ghosh, M., Huynh, D. L., Lee, S. J., Min, T., Kwon, T., & Jeong, D. K. (2017). Nanoformulations of curcumin: An emerging paradigm for improved remedial application. *Oncotarget*, *8*(39), 66680–66698. https://doi.org/10.18632/oncotarget.19164

Grimm, S., Mvondo, D., Grune, T., & Breusing, N. (2011). The outcome of 5-ALA-mediated photodynamic treatment in melanoma cells is influenced by vitamin C and heme oxygenase-1. *BioFactors (Oxford, England)*, *37*(1), 17–24. https://doi.org/10.1002/biof.129

Hadjur, C., Richard, M.-J., Parat, M.-O., Jardon, P., & Favier, A. (1996). Photodynamic effects of hypericin on lipid peroxidation and antioxidant status in melanoma cells. *Photochemistry and Photobiology*, *64*(2), 375–381. https://doi.org/10.1111/j.1751-1097.1996.tb02474.x

Hosseinzadeh, R., Khorsandi, K., & Hosseinzadeh, G. (2018). Graphene oxide-methylene blue nanocomposite in photodynamic therapy of human breast cancer. *Journal of Biomolecular Structure and Dynamics*, *36*(9), 2216–2223. https://doi.org/10.1080/07391102.2017.1345698

Hosseinzadeh, R., & Moosavi-Movahedi, A. A. (2016). Human hemoglobin structural and functional alterations and heme degradation upon interaction with benzene: A spectroscopic study. *Spectrochimica Acta*

Part A: Molecular and Biomolecular Spectroscopy, *157*, 41–49. https://doi.org/10.1016/j.saa.2015.12.014

Huang, Y.-Y., Vecchio, D., Avci, P., Yin, R., Garcia-Diaz, M., & Hamblin, M. R. (2013). Melanoma resistance to photodynamic therapy: New insights. *Biological Chemistry*, *394*(2), 239–250. https://doi.org/10.1515/hsz-2012-0228

Jilaveanu, L. B., Aziz, S. A., & Kluger, H. M. (2009). Chemotherapy and biologic therapies for melanoma: Do they work? *Clinics in Dermatology*, *27*(6), 614–625. https://doi.org/10.1016/j.clindermatol.2008.09.020

Keyvani-Ghamsari, S., Khorsandi, K., & Gul, A. (2020). Curcumin effect on cancer cells' multidrug resistance: An update. *Phytotherapy Research*. Retrieved from https://doi.org/10.1002/ptr.6703

Khorsandi, K., Hosseinzadeh, R., & Fateh, M. (2015). Curcumin intercalated layered double hydroxide nanohybrid as a potential drug delivery system for effective photodynamic therapy in human breast cancer cells. *RSC Advances*, *5*(114), 93987–93994. https://doi.org/10.1039/C5RA15888E

Khorsandi, K., Hosseinzadeh, R., & Shahidi, F. K. (2019). Photodynamic treatment with anionic nanoclays containing curcumin on human triple-negative breast cancer cells: Cellular and biochemical studies. *Journal of Cellular Biochemistry*, *120*(4), 4998–5009. https://doi.org/10.1002/jcb.27775

Kruger, C., & Abrahamse, H. (2018). Utilisation of targeted nanoparticle photosensitiser drug delivery systems for the enhancement of photodynamic therapy. *Molecules*, *23*(10), 2628. https://doi.org/10.3390/molecules23102628

Lincoln, R., Kohler, L., Monro, S., Yin, H., Stephenson, M., Zong, R., Chouai, A., Dorsey, C., Hennigar, R., Thummel, R. P., & McFarland, S. A. (2013). Exploitation of Long-Lived 3IL excited states for metal-organic photodynamic therapy: Verification in a metastatic melanoma model. *Journal of the American Chemical Society*, *135*(45), 17161–17175. https://doi.org/10.1021/ja408426z

Messori, L., Gabbiani, C., Casini, A., Siragusa, M., Vincieri, F. F., & Bilia, A. R. (2006). The reaction of artemisinins with hemoglobin: A unified picture. *Bioorganic & Medicinal Chemistry*, *14*(9), 2972–2977. https://doi.org/10.1016/j.bmc.2005.12.038

Moreno-Vega, A.-I., Gómez-Quintero, T., Nuñez-Anita, R.-E., Acosta-Torres, L.-S., & Castaño, V. (2012). Polymeric and ceramic nanoparticles in biomedical applications. *Journal of Nanotechnology*, *2012*, 1–10. https://doi.org/10.1155/2012/936041

Nafisi, S., Adelzadeh, M., Norouzi, Z., & Sarbolouki, M. N. (2009). Curcumin binding to DNA and RNA. *DNA and Cell Biology*, *28*(4), 201–208. https://doi.org/10.1089/dna.2008.0840

Naidoo, C., Kruger, C. A., & Abrahamse, H. (2018). Photodynamic therapy for metastatic melanoma treatment: A review. *Technology in Cancer Research & Treatment*, *17*, 1533033818791795. https://doi.org/10.1177/1533033818791795

Naksuriya, O., Okonogi, S., Schiffelers, R. M., & Hennink, W. E. (2014). Curcumin nanoformulations: A review of pharmaceutical properties and preclinical studies and clinical data related to cancer treatment. *Biomaterials*, *35*(10), 3365–3383. https://doi.org/10.1016/j.biomaterials.2013.12.090

Nobili, S., Lippi, D., Witort, E., Donnini, M., Bausi, L., Mini, E., & Capaccioli, S. (2009). Natural compounds for cancer treatment and prevention. *Pharmacological Research*, *59*(6), 365–378. https://doi.org/10.1016/j.phrs.2009.01.017

Palumbo, G. (2007). Photodynamic therapy and cancer: A brief sightseeing tour. *Expert Opinion on Drug Delivery*, *4*(2), 131–148. https://doi.org/10.1517/17425247.4.2.131

Paunovic, V., Ristic, B., Markovic, Z., Todorovic-Markovic, B., Kosic, M., Prekodravac, J., Kravic-Stevovic, T., Martinovic, T., Micusik, M., Spitalsky, Z., Trajkovic, V., & Harhaji-Trajkovic, L. (2016). c-Jun N-terminal kinase-dependent apoptotic photocytotoxicity of solvent exchange-prepared curcumin nanoparticles. *Biomedical Microdevices*, *18*(2), 37. https://doi.org/10.1007/s10544-016-0062-2

Riggs, A. (1981). Preparation of blood hemoglobins of vertebrates. E. Antonini, L. Rossi-Bernardi, & E. Chiancone (Eds.), *Methods in Enzymology* (pp. 5–29). Elsevier. https://doi.org/10.1016/0076-6879(81)76111-1

Santezi, C., Reina, B. D., & Dovigo, L. N. (2018). Curcumin-mediated photodynamic therapy for the treatment of oral infections – A review. *Photodiagnosis and Photodynamic Therapy*, *21*, 409–415. https://doi.org/10.1016/j.pdpdt.2018.01.016

Siegel, R. L., Miller, K. D., & Jemal, A. (2019). Cancer statistics, 2019. *CA: A Cancer Journal for Clinicians*, *69*(1), 7–34. https://doi.org/10.3322/caac.21551

Singh, S. P., Sharma, M., & Gupta, P. K. (2015). Evaluation of phototoxic effects of curcumin loaded in organically modified silica nanoparticles in tumor spheroids of oral cancer cells. *BioNanoScience*, *5*(1), 10–21. https://doi.org/10.1007/s12668-014-0157-2

Sweeting, L. M. (1998). Organic structural spectroscopy (Lambert, Joseph B.; Shurvell, Herbert F.; Lightner, David A.; Cooks, R. Graham). *Journal of Chemical Education*, *75*(10), 1218. https://doi.org/10.1021/ed075p1218

Tampa, M., Sarbu, M.-I., Matei, C., Mitran, C.-I., Mitran, M.-I., Caruntu, C., Constantin, C., Neagu, M., & Georgescu, S.-R. (2019). Photodynamic therapy: A hot topic in dermato-oncology (Review). *Oncology Letters*, *17*(5), 4085–4093. Retrieved from https://doi.org/10.3892/ol.2019.9939

Tu, B., Chen, Z.-F., Liu, Z.-J., Cheng, L.-Y., & Hu, Y.-J. (2015). Interaction of flavones with DNA in vitro: structure-activity relationships. *RSC Advances*, *5*(42), 33058–33066. Retrieved from https://doi.org/10.1039/C5RA04505C. [1]

Verwanger, T., Krammer, B., & Bernardinelli, E. (2011). Curcumin as a photosensitizer: Studies on different cell lines. *Photodiagnosis and Photodynamic Therapy*, *8*(2), 186. https://doi.org/10.1016/j.pdpdt.2011.03.216

Xiao, L., Gu, L., Howell, S. B., & Sailor, M. J. (2011). Porous silicon nanoparticle photosensitizers for singlet oxygen and their phototoxicity against cancer cells. *ACS Nano*, *5*(5), 3651–3659. https://doi.org/10.1021/nn1035262

Xu, X.-Y., Meng, X., Li, S., Gan, R.-Y., Li, Y., & Li, H.-B. (2018). Bioactivity, health benefits, and related molecular mechanisms of curcumin: Current progress, challenges, and perspectives. *Nutrients*, *10*(10), 1553. https://doi.org/10.3390/nu10101553

Yi, G., Hong, S. H., Son, J., Yoo, J., Park, C., Choi, Y., & Koo, H. (2018). Recent advances in nanoparticle carriers for photodynamic therapy. *Quantitative Imaging in Medicine and Surgery*, *8*(4), 433–443. https://doi.org/10.21037/qims.2018.05.04